ISCI, Volume *2*

Supplemental Information

Adaptive Regulation of Nitrate Transceptor NRT1.1 in Fluctuating Soil Nitrate Conditions

Mubasher Rashid, Soumen Bera, Alexander B. Medvinsky, Gui-Quan Sun, Bai-Lian Li, and Amit Chakraborty

Supplemental figures and legends

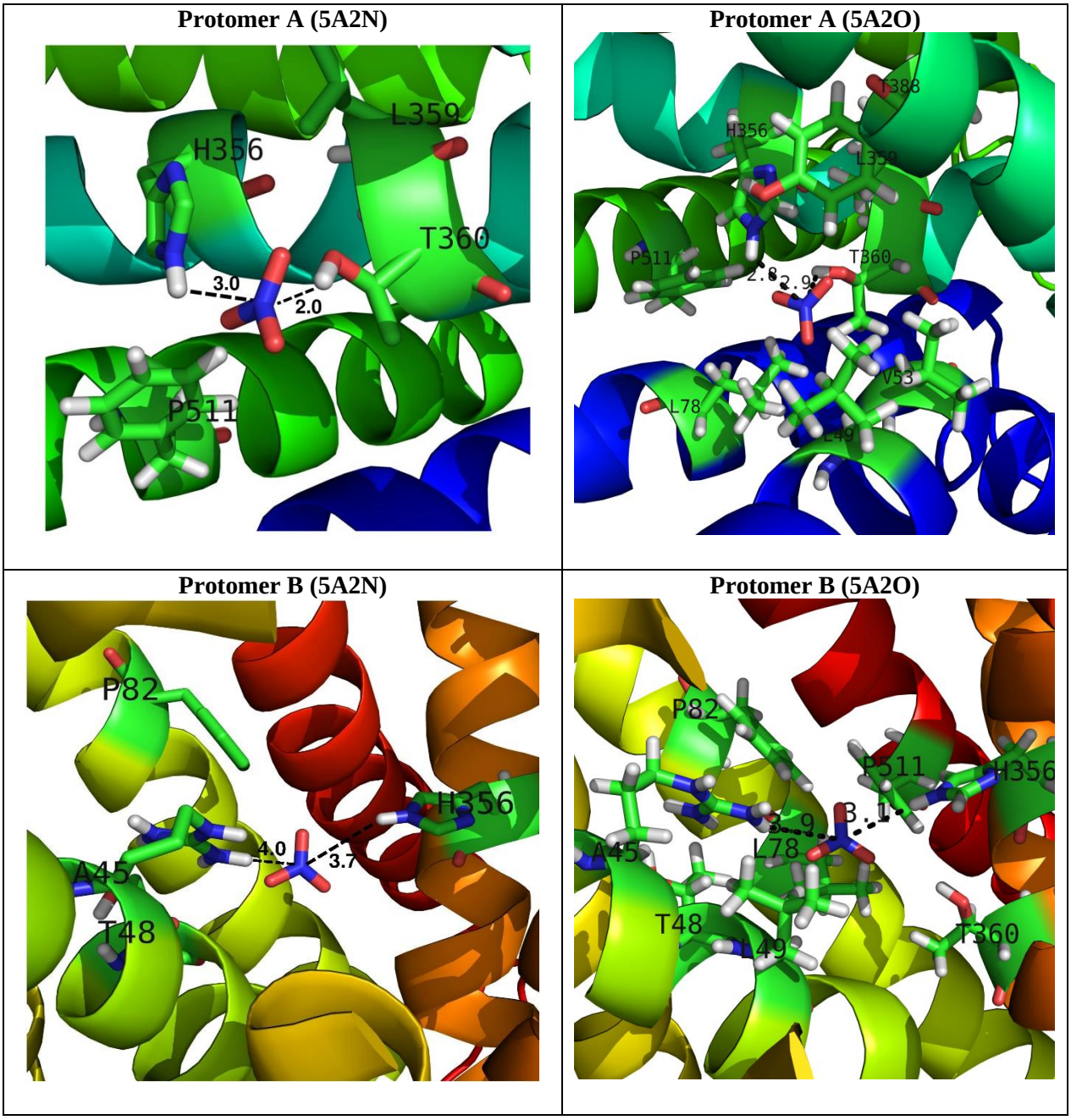

Figure S1. Close up of neighbourhood residue compositions around nitrate within the distance of 4.0 Å, related to Figure 1 and interprotomer asymmetries. It shows differential neighbourhood compositions between the protomers.

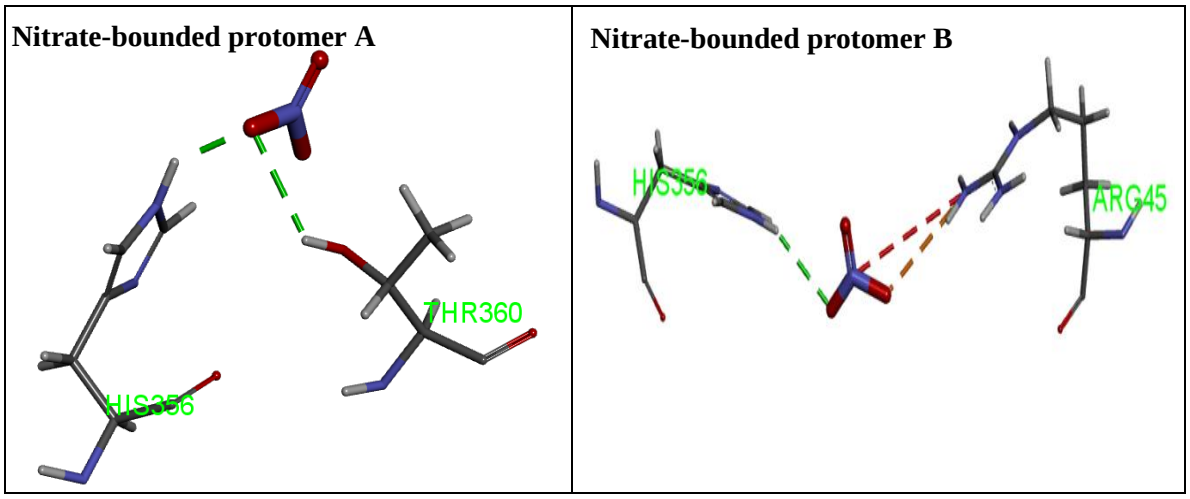

Figure S2. H-bond interactions between nitrate and amino acid residues in protomers A and B, related to Figure 1 and interprotomer asymmetries and differential nitrate-binding affinities. Nitrate interacts with HIS 356 and THR 360 in the nitrate bounded protomer A, whereas it interacts with HIS 356 and ARG 45 in the protomer B.

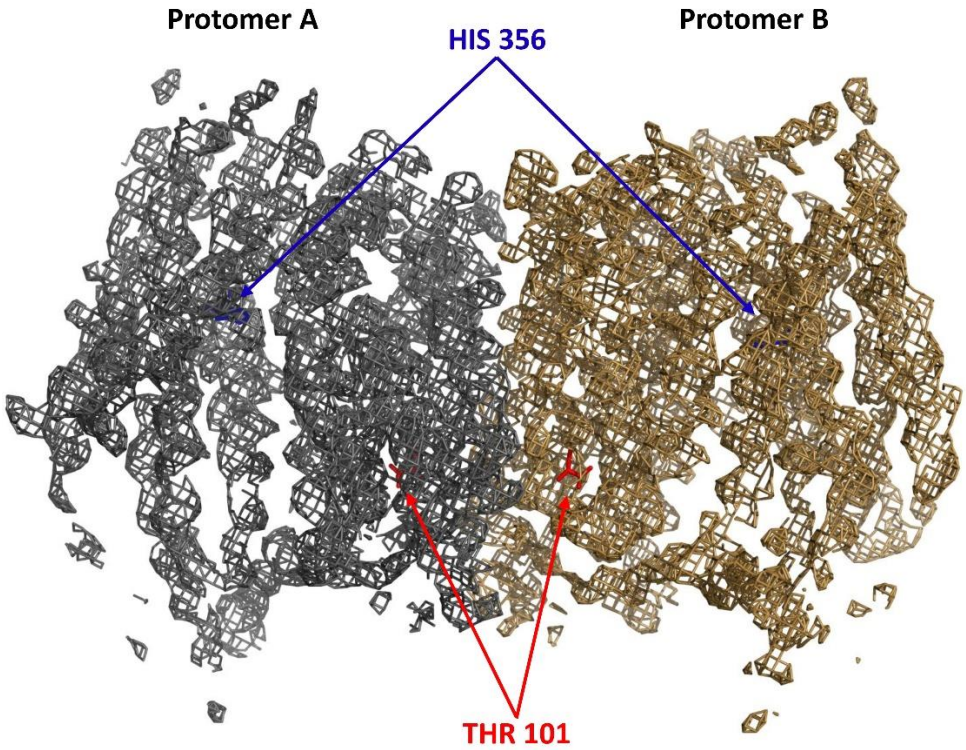

Figure S3. View of $2F_o$ - F_c density map contoured at 2.0 δ, related to Figure 2 and interprotomer asymmetries. It shows the local asymmetry at nitrate binding site residue (blue arrow) and phosphorylation site residue (red arrow).

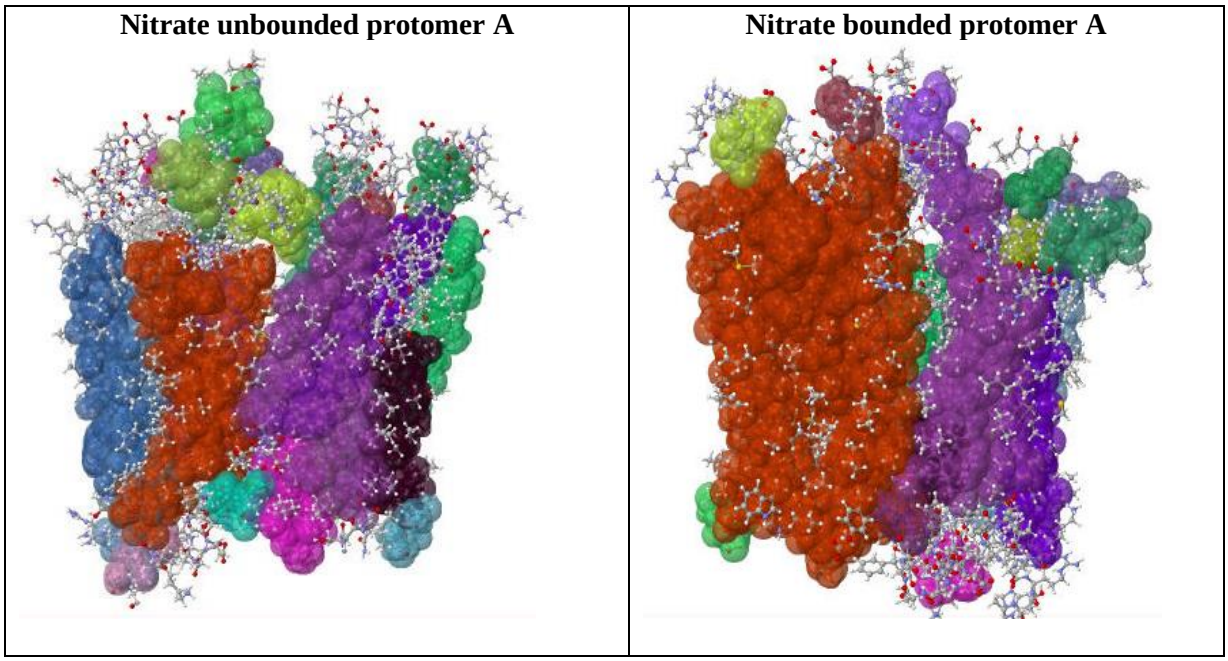

Figure S4. Comparison of rigid cluster distribution in protomer A of NRT1.1, related to Figure 4 and intraprotomer allosteric communications. Red colour denotes largest rigid cluster. This rigid cluster becomes even more large in nitrate bounded protomer A containing residues [30, 94] spanning between nitrate binding pocket and Thr 101 site.

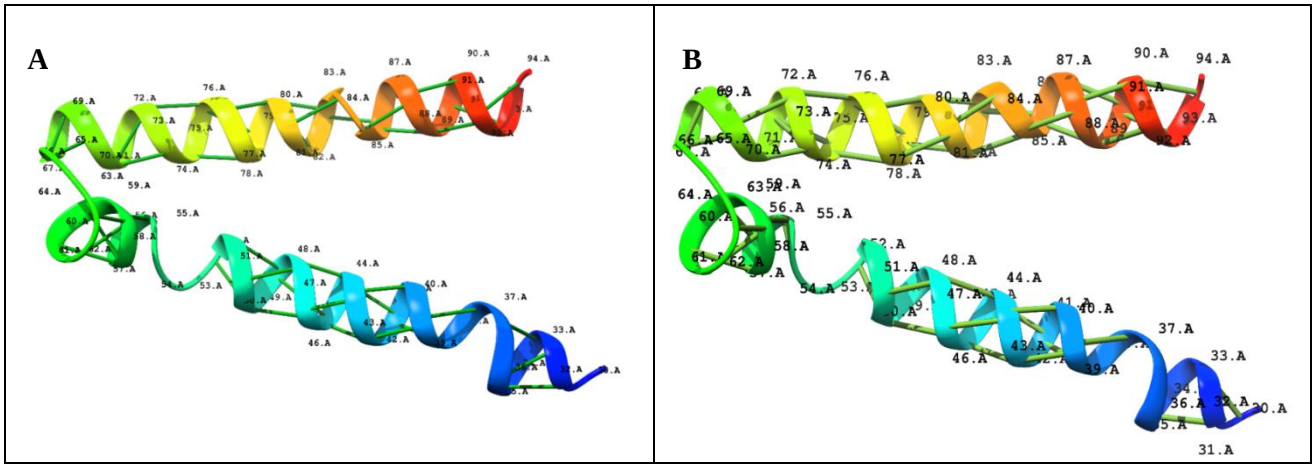

Figure S5. Visual illustration of distribution of H-bonds, related to Figure 5 and intraprotomer allosteric communications. Nitrate unbounded protomer A (A), and nitrate bounded protomer A (B) in the residue range [30, 94]. After nitrate binding (B) there is redistribution of hydrogen bounds and also few more hydrogen bonds are added in this cluster.

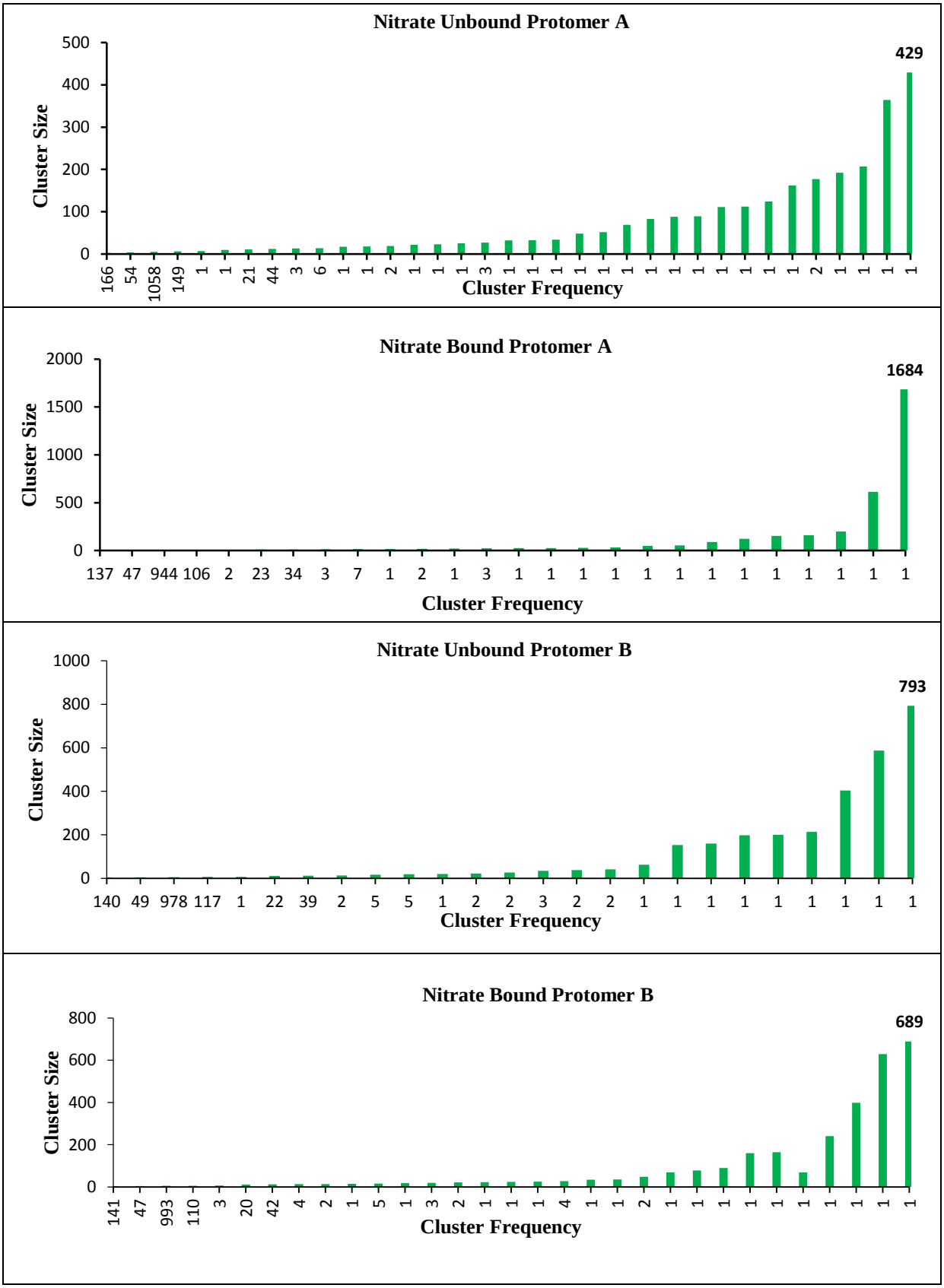

Figure S6. Bar graphs display frequency and size of rigid clusters in apo and nitrate bounded protomers of NRT1.1., related to Figure 4 and intraprotomer allosteric communications. In nitrate bound protomer A, there is a large cluster consisting of 1684 atoms which spans between nitrate binding site and Thr101 site. However no such cluster has been found in any of the other protomers.

Supplemental tables

Table S1: Compositional differences between the nitrate-bounded and unbounded NRT1.1, related to Figure 2 and interprotomer asymmetries.

	NRT1.1 apo-protein (5A2N)		NRT1.1 nitrate-bounded protein (5A2O)	
	Nitrate neighbourhood (4.0 Å)	**Thr101 neighbourhood (4.0 Å)**	**Nitrate neighbourhood (4.0 Å)**	**Thr101 neighbourhood (4.0 Å)**
Protomer A	Leu 49, His 356, Leu 359, Thr 360, Tyr 388, Phe 511	Gly 88, Ile 91, Ala 92, Gly 97, Arg 98, Tyr 99, Leu 100, Ile 102, Ala 103, Ile 104, Phe 105, Gly 162, Ser 166	Leu 49, Val 53, Leu 78, His 356, Leu 359, Thr 360, Tyr 388, Phe 511	Gly 88, Ile 91, Ala 92, Gly 97, Arg 98, Tyr 99, Leu 100, Ile 102, Ala 103, Ile 104, Phe 105, Ala 106, Gly 162, Val 163, Ser 166
Protomer B	Arg 45, Thr 48, Leu 49, Phe 82, His 356	Gly 88, Ile 91, Ala 92, Gly 97, Arg 98, Tyr 99, Leu 100, Ile 102, Ala 103, Ile 104, Phe 105, Ala 106, Gly 162, Val 163, Ala 165, Ser 166	Arg 45, Thr 48, Leu 49, Leu 78, Phe 82, His 356, Thr 360, Phe 511	Gly 88, Ile 91, Ala 92, Gly 97, Arg 98, Tyr 99, Leu 100, Ile 102, Ala 103, Ile 104, Phe 105, Ala 106, Gly 162, Val 163, Ala 165, Ser 166

Table S2: Summary of changes in allowed regions of dihedral angles, related to Figure 1.

Nitrate unbounded protomer A	Nitrate bounded protomer A	Nitrate unbounded protomer B	Nitrate bounded protomer B
HIS 356 (-58.62, -46.40)	**HIS356 (-76.65, -30.76)**	**HIS 356 (-77.36, -27.82)**	**HIS 356 (-71.49, -35.86)**
THR 360 (-80.38, -31.38)	**THR 360 (-77.17, -40.27)**	**ARG 45 (-55.82, -40.33)**	**ARG 45 (-63.89, -67.96)**
THR 101 (-59.49, -47.27)	**THR 101 (-62.12, -31.32)**	**THR 101 (-63.87, -36.67)**	**THR 101 (-68.20, -41.31)**

Table S3: Interface statistics, related to Figure 3.

	NRT1.1 Apo-protein (5A2N)			NRT1.1 nitrate-bounded protein (5A2O)		
	Interface area ($Å^2$)	**No. of interface residues**	**No. of hydrogen bonds**	**Interface area ($Å^2$)**	**No. of interface residues**	**No. of hydrogen bonds**
Protomer A	**1093**	**21**	**04** **Thr111 --Val229** **Thr111--Ser233** **Thr111--Ser233** **Val229--Thr11**	**1087**	**20**	**01** **Ser233--Thr111**
Protomer B	**1099**	**23**		**1078**	**21**	

Table S4: Summary of mutational analysis, related to Figure 7 and *in silico* mutational analysis					
Mutation [80-90]	**Cluster Break(Y/N)**	**No. of clusters formed**	**No. of h-bonds in the allosteric rigid cluster [30-94]**	**ΔΔG (Mutant -WT) Kcal/mol**	**Stability**
Thr101Asp **(T101D)**	N	1	53	2.45	Highly Destabilizing
Thr101Ala **(T101A)**	Y	2	53	0.45	Neutral
Thr80Ala	N	1	55	-0.83	Slightly Stabilizing
Thr80Asp	N	1	53	-0.18	Neutral
Thr80His	N	1	55	-0.97	Stabilizing
Thr80Leu	Y	2	54	-2.38	Highly Stabilizing
Thr80Pro	N	1	52	4.26	Highly Destabilizing
Thr80Ser	Y	2	55	-0.38	Neutral
Thr80Val	N	1	54	-0.63	Slightly Stabilizing
Ser81Ala	N	1	55	-0.39	Neutral
Ser81Asp	Y	2	53	3.33	Highly Destabilizing
Ser81His	N	1	53	3.61	Highly Destabilizing
Ser81Leu	N	1	55	1.27	Destabilizing
Ser81Pro	N	1	53	4.65	Highly Destabilizing
Ser81Thr	Y	2	56	0.89	Slightly Destabilizing
Ser81Val	Y	2	53	0.59	Slightly Destabilizing
Leu84Ala	N	1	55	1.91	Highly Destabilizing
Leu84Asp	Y	2	57	3.26	Highly Destabilizing
Leu84His	N	1	54	1.01	Destabilizing
Leu84Pro	Y	2	54	6.11	Highly Destabilizing
Leu84Ser	N	1	54	2.74	Highly Destabilizing
Leu84Thr	Y	2	55	1.64	Destabilizing
Leu84Val	N	1	55	0.40	Neutral

Transparent Methods

Visual analysis of neighbourhoods

Comparative visual analyses of apo- and nitrate bounded crystallographic structures presents the differences in 4.0 Å neighbourhoods of nitrate and Thr101 phosphorylation site (Table S1). Nitrate and Thr101 neighbourhoods have been determined by using PyMOL v1.7.2.1 (DeLano, 2006). To determine nitrate neighbourhoods in nitrate-unbounded protomers of apo-protein, nitrate has been separated from the two protomers of nitrate bounded crystallographic structure in PyMOL and then superimposed in the respective unbounded protomers of apo-protein.

Interactions of nitrate in the binding sites of two protomers of NRT1.1 have been determined in UCSF Chimera (version 1.11.2) (Pettersen et al., 2004). It was further verified in BIOVIA Discovery Studio v16.1.0. While in protomer A, nitrate showed interactions with the residues His 356 and Thr 360, in protomer B Thr 360 was replaced by Arg 45 (Figure S1, S2). These residues are also in close proximity to nitrate among other neighbouring residues.

Visual analysis shows that in protomer A of NRT1.1, residues Thr 360 and His 356 are in close proximity to nitrate, while as in protomer B residues Arg 45 and His 356 are closer to nitrate. Ramachandran plot (Ramachandran et al., 1963) has been used to illustrate the changes in energetically allowed regions of the backbone dihedral angles. In particular comparative analysis using Visual Molecular Dynamics (version 1.9.3beta4) (Humphrey et al., 1996) has identified significant changes in allowed regions of Phi and Psi angles in the residues Thr360, His 356, Arg45, and the phosphorylation site Thr101 before and after nitrate binding (Table S2).

We have used PDBePISA (www.ebi.ac.uk/pdbe/pisa), a web-based interactive tool, for analysing the interfaces between the protomers of NRT1.1 nitrate-unbounded and bounded crystals. The interface of apo-structure with the interfacing area A.1093 Å² and B.1099 Å², besides the non-bonded contacts, the only bonded contacts present are four hydrogen bonds: A.Thr111 --B.Val229, A.Thr111--B.Ser233, A.Thr111--B.Ser233, A.Val229--B.Thr11. After nitrate binding, all the four interactions are completely lost with reduced interfacing surface area, building a single new H-bond between A.Ser233-B.Thr111 (Table S3).

Electron Density Map

To examine the intrinsic local structural asymmetry between the two protomers in the asymmetric units, we used CCP4 maps (Jones et al., 1991; Winn et al., 2011) to produce $2F_o$-F_c electron density map contoured at 2.0 σ (Figure S3). A closed view at the binding site (blue) and phosphorylation site (red) of the two protomers shows different conformations of the residues involving these sites. While His 356 in protomer A and Thr 101 in protomer B surfaced out, His 356 in protomer B and Thr 101 in protomer A are comparatively buried. We have also observed that this asymmetry is sustained and further differentially enhanced after nitrate binding.

Chemical shifts

To predict differences in chemical shifts between the nitrate bounded and unbounded protomers, SHIFTX2 (http://www.shiftx2.ca) has been used with inputs of apo-and nitrate bounded crystal structures of *Arabidopsis thaliana* NRT1.1. It correlates intrinsic interprotomer asymmetry with the nitrate-bounded states, with the differences between backbone chemical shifts, $^{13}C\alpha\ \Delta\delta$, of protomers A and B. It shows a wide range of variation for both the protomers A (0.003-3.6 ppm) and B (0.003-4.0 ppm). SHIFTX2 combines ensemble machine learning methods with sequence alignment-based methods.

Rigidity Analysis

Molecular theorem and protein rigidity

Molecular theorem is the key result used in *pebble game algorithm* to determine the rigidity/flexibility predictions of protein structures by analysing their underlying graphs. For molecular structures, the underlying graph is a simple graph G_M= (V, H_M) where V is the vertex set consisting of bodies of atoms and H_M is the set of molecular hinges around which bodies are free to rotate. Each body is a collection of atoms connected by chemical interactions like double or non-rotatable bonds such that the atoms do not move individually with respect to each other, rather they all move together as a single body. Such bodies of atoms in 3-D have 6 degrees of freedom (three translations and three rotations). Also each hinge between two bodies removes five degrees of freedom (DOF). Replacing bodies with vertices and each hinge with five bars (edges), a body hinge framework becomes a multigraph. Molecular theorem stated below checks the rigidity of multigraph by looking into the rigidity of each of its subgraph.

Theorem (generic): A molecular structure on a graph G_M = (V, H_M) is rigid iff each molecular hinge is replaced by 5 edges, the resulting multigraph G = (V, E) has 6|V| -6 edges and for every non empty set $E' \subseteq$ E with V' vertices, $|E'| \leq 6|V'| - 6$.

Rigidity-based allostery is examined using KINARI software (Fox et al., 2011) that uses pebble game algorithm for classifying the whole protein structure into rigid clusters of different sizes. The distribution of rigid clusters (Figure S4, S6) within protomer A and protomer B indicates the relative flexibility of protomer B. The largest rigid cluster in nitrate bounded protomer A contains total 1684 atoms within the AA residues 30-94 with X_{LRC} = N_{LRC}/N = 0.23 (where N is the total number of atoms in protomer A and N_{LRC} is the total number of atoms in the largest rigid cluster (LRC) in protomer A). This largest cluster involves part of the residues of the neighbourhood of 4.0 A of nitrate binding site and the Thr101 site. To determine fraction of nitrate binding site and Thr 101 site residues in largest rigid cluster in either of the apo and nitrate bound protomers, we calculated

$Z_{LRC}^{A,\,NO_3-unbounded} = 0.24, Z_{LRC}^{A,\,NO_3-bounded} = 0.12\ such\ that\ \Delta Z_{LRC}^{A} = 0.12 > 0\ and\ Z_{LRC\_T101}^{A,\,NO_3-unbounded} = 0.52, Z_{LRC\_T101}^{A,\,NO_3-bounded} = 0.23\ such\ that\ \Delta Z_{LRC\_T101}^{A} = 0.29 >$ **0**.

Positive values of these expressions indicate that nitrate binding is the main source of change in rigidity of protomers **(**Rader and Brown 2010**).** In contrast, there doesn't exits such largest rigid cluster for allostery in protomer B. This theoretical analysis, therefore, suggests that

nitrate-induced conformational changes establish a rigidity-based allosteric communications between the nitrate-binding site and the Thr 101 site that is responsible for priming Thr 101 for phosphorylation.

Mutational Analysis

Noting that most of the new H-bonds in protomer A have been added within the residue range 80-90, AA residues have been chosen from this region for mutational analysis. Nitrate-bound protomer A has been separated from the pdb file (PDB id: 5a2o), repaired in FoldX **(**Schymkowitz et al., 2005**)** to identify and fix bad torsion angles, Vander Waal's clashes so as to complete the structure. This molecule is then taken as input in the UCSF Chimera. Using the mutation tool box (Rotamer), selected single amino acid residue is replaced by the observed or potential residue and then whole protein molecule energy-minimization is carried out in 300 steps with the method of steepest descent minimization to relieve highly unfavourable clashes followed by conjugate gradient minimization. Rigidity-based allosteric analysis has been carried out on this mutated molecule in the KINARI software. Further, the energetic impact of mutations on protein stability is estimated using FoldX, which calculates $\Delta\Delta G$ by using formula $\Delta\Delta G_{fold} = \Delta G_{fold,\ mut} - \Delta G_{fold,\ wt}$. By using method as employed in Studer et al.(2014), we categorized the stabilities of mutants on the basis of their $\Delta\Delta G$ values (Table S5).

To identify key residues in allosteric communication pathway [30-94], all possible *in-silico* mutational analyses have been carried out in protomer A of the NRT1.1 crystallographic structure. This method is calibrated with the experimental results of Ho et al. (2009) in which single amino acid mutants Thr101Asp (T101D) and Thr101Ala (T101A) mimicked as phosphorylated and de-phosphorylated states of NRT1.1, respectively. In parallel to this experimental result, it has been observed that T101A breaks the rigid cluster that is responsible for allosteric communication into two distinct clusters, whereas the T101D retains the intact allosteric rigid cluster. It therefore suggests that priming of T101 site in protomer A for the phosphorylation is allosterically triggered by the high-affinity nitrate-binding, whereas in protomer B such allosteric communication is weak or absent. The analysis showed that Ser 81 is one of the potential key residues for maintaining the allosteric communication pathway. With the mutations of Ser81Thr, Ser81Val, and Ser81Asp, the allosteric rigid-cluster splits into two distinct clusters due to the loss of H-bonds between Ser 81 and Phe 77, and Ser 81 and Cys 85 which were added through nitrate-binding.

Supplemental references

Fox, N., Jagodzinski, F., Li, Y., and Streinu, I. (2011). KINARI-Web: A server for protein rigidity analysis. *Nucleic Acids Research* 39, 177–183.

Humphrey, W., Dalke, A., and Schulten, K. (1996).VMD - Visual Molecular Dynamics. *Journal of Molecular Graphics* 14, 33-38.

Jones, T.A., Zou, J.Y., Cowan, S.W., and Kjeldgaard, M. (1991). Improved methods for building models in electron density maps and the location of errors in these models. *Acta Crystallographica Section A* 47, 110–119.

Pettersen, E.F., Goddard, T.D., Huang, C.C., Couch, G.S., Greenblatt, D.M., Meng, E.C., and Ferrin, T.E.(2004) UCSF Chimera - a visualization system for exploratory research and analysis. *Journal of Computational Chemistry* 25, 1605-1612.

Ramachandran, G. N., Ramakrishnan, C., and Sasisekharan, V. (1963). Stereochemistry of polypeptide protomer configurations. *Journal of Molecular Biology* 7, 95–99.

Schymkowitz, J., Borg, J., Stricher, F., Nys, R., Rousseau, F., and Serrano, L. (2005). The FoldX web server: an online force field. *Nucleic Acids Research* 33, 382 – 388.

Studer, R.A., Christin, P.A., Williams, M.A., Orengo, C.A. (2014). Stability-activity tradeoffs constrain the adaptive evolution of RubisCO. *Proc. Nat. Acad. Sc. (USA)* 111, 2223–2228.

Winn, M.D., Ballard, C.C., Cowtan, K.D., Dodson, E.J., Emsley, P., Evans, P.R., Keegan, R.M., Krissinel, E.B., Leslie, A.G., McCoy, A., McNicholas, S.J., Murshudov, G.N., Pannu, N.S., Potterton, E.A., Powell, H.R., Read, R.J., Vagin, A., and Wilson, K.S. (2011). Overview of the CCP4 suite and current developments. *Acta Crystallographica Section D* 67, 235–242.